TRICHOME BIREFRINGENCE and Its Homolog *AT5G01360* Encode Plant-Specific DUF231 Proteins Required for Cellulose Biosynthesis in Arabidopsis[1][W][OA]

Volker Bischoff[2]*, Silvia Nita[2], Lutz Neumetzler, Dana Schindelasch, Aurélie Urbain, Ravit Eshed, Staffan Persson, Deborah Delmer[3], and Wolf-Rüdiger Scheible

Max Planck Institute of Molecular Plant Physiology, 14476 Potsdam, Germany (V.B., S.N., L.N., D.S., S.P., W.-R.S.); Institut Jean-Pierre Bourgin, UMR 1318 INRA-AgroParisTech, INRA Centre de Versailles-Grignon, 78026 Versailles, France (V.B., A.U.); Department of Ornamental Horticulture, The Volcani Center, Agricultural Research Organization, Bet Dagan 50250, Israel (R.E.); and Section of Plant Biology, University of California, Davis, California 95616 (D.D.)

The Arabidopsis (*Arabidopsis thaliana*) *trichome birefringence* (*tbr*) mutant has severely reduced crystalline cellulose in trichomes, but the molecular nature of *TBR* was unknown. We determined *TBR* to belong to the plant-specific DUF231 domain gene family comprising 46 members of unknown function in Arabidopsis. The genes harbor another plant-specific domain, called the TBL domain, which contains a conserved GDSL motif known from some esterases/lipases. *TBR* and *TBR-like3* (*TBL3*) are transcriptionally coordinated with primary and secondary *CELLULOSE SYNTHASE* (*CESA*) genes, respectively. The *tbr* and *tbl3* mutants hold lower levels of crystalline cellulose and have altered pectin composition in trichomes and stems, respectively, tissues generally thought to contain mainly secondary wall crystalline cellulose. In contrast, primary wall cellulose levels remain unchanged in both mutants as measured in etiolated *tbr* and *tbl3* hypocotyls, while the amount of esterified pectins is reduced and pectin methylesterase activity is increased in this tissue. Furthermore, etiolated *tbr* hypocotyls have reduced length with swollen epidermal cells, a phenotype characteristic for primary *cesa* mutants or the wild type treated with cellulose synthesis inhibitors. Taken together, we show that two *TBL* genes contribute to the synthesis and deposition of secondary wall cellulose, presumably by influencing the esterification state of pectic polymers.

As the major component of the plant cell wall, cellulose has diverse functions. In the primary wall, cellulose is important for the production of the cell plate during cell division, for anisotropic cell expansion, and for turgor pressure distribution (Shedletzky et al., 1992). Thus, the cellulose microfibrils largely determine cell shape and patterns of development (Carpita and McCann, 2000). Once plant cells have stopped expanding, some cell types deposit a secondary cell wall (Taylor et al., 2000) that is mainly composed of highly aligned, crystalline cellulose microfibrils, noncellulosic polysaccharides, such as xylans and mannans (Carpita and McCann, 2000; Ebringerova and Heinze, 2000; Brown et al., 2005), and lignin. These polymers provide a framework that gives further strength to cells that have to sustain enhanced mechanical stress. Secondary cell walls are the major components in wood and plant fibers, underlining their economical importance (Brown et al., 2005). Cell walls are also important for protecting cells against pathogens, dehydration, or other environmental factors (Braam, 1999; Jones and Takemoto, 2004; Vorwerk et al., 2004).

More than 1,000 genes in the Arabidopsis (*Arabidopsis thaliana*) genome are estimated to encode cell wall-related proteins, but the specific biological contexts and the biochemical functions of most of these proteins are largely unknown (Carpita et al., 2001; Somerville et al., 2004). The first plant *CELLULOSE SYNTHASE* (*CESA*) genes were identified in cotton (*Gossypium hirsutum*) through sequence homology to conserved regions of bacterial cellulose synthases and high expression levels coinciding with high rates of cellulose synthesis (Pear et al., 1996). A family of *CESA*-related genes was rapidly identified in Arabidopsis, and their function as cellulose synthases was subsequently corroborated by classical genetic approaches (Arioli et al., 1998; Taylor et al., 1999, 2000; Fagard et al., 2000). Mutants in primary *CESA* genes generally contain strongly reduced levels of cellulose and exhibit

[1] This work was supported by the German Science Foundation (grant no. SCHE 548/2), the Max Planck Society, and the European Union Framework Program 6 (Cellulose Architecture Systems Biology for Plant Innovation Creation grant no. NEST–CT–2004–028974 to V.B.).

[2] These authors contributed equally to the article.

[3] Present address: 33 Riverside Dr., New York, NY 10023.

* Corresponding author; e-mail volker.bischoff@versailles.inra.fr.

The author responsible for distribution of materials integral to the findings presented in this article in accordance with the policy described in the Instructions for Authors (www.plantphysiol.org) is: volker.bischoff@versailles.inra.fr.

[W] The online version of this article contains Web-only data.

[OA] Open Access articles can be viewed online without a subscription.

www.plantphysiol.org/cgi/doi/10.1104/pp.110.153320

dwarfed growth phenotypes (Arioli et al., 1998; Fagard et al., 2000; Burn et al., 2002). Mutants in secondary *CESA* genes, on the other hand, show characteristic irregular xylem vessels (Taylor et al., 1999, 2000), a phenotype that subsequently also has been reported for other secondary cell wall mutants (Brown et al., 2005). Besides the CESAs, several other components are believed to participate in cellulose deposition, such as the endo-1,4-β-D-glucanase KORRIGAN (Nicol et al., 1998), the glycophosphatidyl inositol-anchored plant-specific COBRA protein (Schindelman, et al., 2001), and the plasma membrane-localized KOBITO1 protein (Pagant et al., 2002; Lertpiriyapong and Sung, 2003). Analysis of Arabidopsis *fragile fiber* (*fra*) mutants, in which interfascicular fibers exhibit reduced mechanical strength, resulted in the identification of mutant alleles for the secondary *CESA* genes (*fra5* and *fra6*; Zhong et al., 2003) but also yielded novel components, some of which presumably are indirectly required for secondary wall synthesis. These include the kinesin-like protein FRA1, which is essential for oriented deposition of cellulose microfibrils and cell wall strength (Zhong et al., 2002), the katanin-like protein FRA2 involved in regulating microtubule disassembly by severing microtubules (Burk et al., 2001), a type II inositol polyphosphate 5-phosphatase (Zhong and Ye, 2004), and the GTP-binding protein RHD3 (Wang et al., 1997; Hu et al., 2003), both required for actin organization in fiber cells. Identification of FRA8 as a putative xylan glucuronyltransferase (Zhong et al., 2005) from the glycosyl transferase (GT) 47 family of carbohydrate-active enzymes (www.cazy.org) points to the importance of acidic xylan (i.e. glucuronoxylan) modifications for normal cellulose deposition during secondary wall formation in Arabidopsis (Reis and Vian, 2004; Peña et al., 2007).

Coexpression analyses of microarray data with *CESA* genes as bait have been used to identify genes associated with cellulose synthesis (Brown et al., 2005; Persson et al., 2005). Mutations in several such genes display cell wall phenotypes characteristic of cellulose deficiency, for example the *COBRA-like* gene *IRREGULAR XYLEM6* (*IRX6*) that contains reduced levels of secondary wall cellulose (Brown et al., 2005). Likewise, the *irx8* and *irx9* mutants display slightly reduced levels in stem secondary wall cellulose (Brown et al., 2005) but appear to be associated with the synthesis of xylans. *IRX8* (*AT5G54690*) and *IRX9* (*AT2G37090*) encode putative glycosyl transferase genes from the GT8 and GT43 families, respectively (www.cazy.org), and were found to be involved in glucuroxylan (GX) synthesis (Bauer et al., 2006; Peña et al., 2007; Persson et al., 2007), suggesting a requirement for normal hemicellulosic polysaccharide synthesis in order for normal secondary wall synthesis and cellulose deposition to occur.

Another important component thought to be required for secondary wall cellulose synthesis is the gene that controls a trait referred to as TRICHOME BIREFRINGENCE (TBR; Potikha and Delmer, 1995). The highly ordered cellulose found in the cell walls of Arabidopsis trichomes displays strong birefringence under polarized light, whereas the Arabidopsis *tbr* mutant displays no such birefringence (Fig. 1), and the cellulose content in *tbr* mutant trichomes is strongly reduced (Potikha and Delmer, 1995). In this work, we report the identification of the gene responsible for the TBR trait and a further characterization of the Arabidopsis *tbr* mutant. We show that *TBR* belongs to a plant-specific, poorly described gene family (*TBR-like* [*TBL*]) with 46 members in Arabidopsis. *TBR* and other gene family members are strongly coexpressed with primary and secondary *CESA* genes, respectively. We further provide evidence that TBR and an additional member of the family influence secondary wall cellulose deposition. Our results also suggest the involvement of the latter genes in pectin modification, more specifically methylesterification, which may affect the deposition of secondary walls.

RESULTS

Novel Phenotypes of the *tbr* Mutant

The *tbr* mutant of Arabidopsis was previously characterized as lacking leaf and stem trichome birefrin-

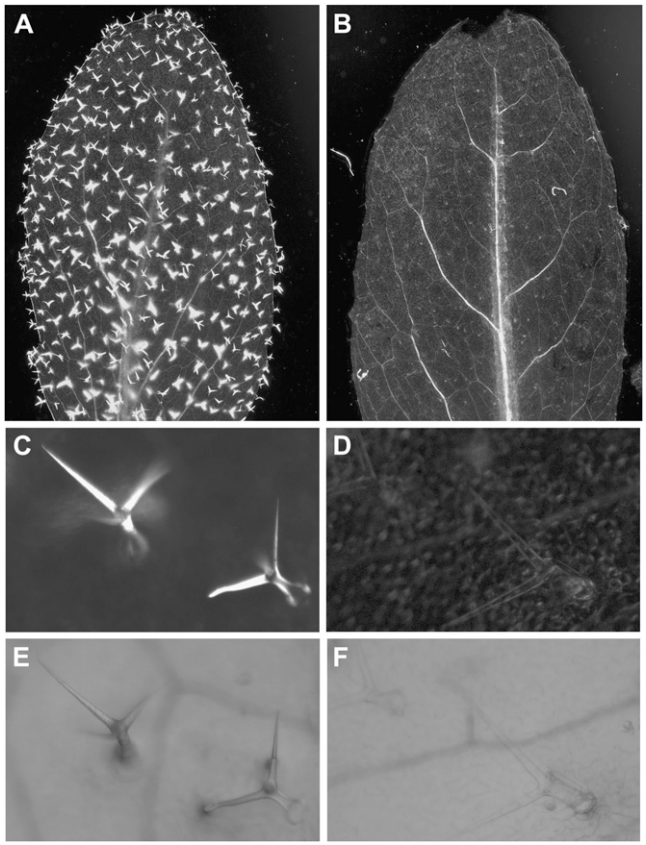

Figure 1. Lack of trichome birefringence in *tbr* mutants. A and B, Birefringence phenotypes of a wild-type Col-0 leaf (A) and a *tbr* mutant leaf (B). C to F, Appearance of individual wild-type and *tbr* mutant trichomes under polarized (C and D) and nonpolarized (E and F) white light.

gence (Potikha and Delmer, 1995; Fig. 1) characteristic of plant cells that contain highly ordered cellulose in their secondary walls. Consistently, cellulose levels were decreased in *tbr* trichomes by greater than 80%. In addition, the cellulose content in the leaf vasculature was decreased approximately 30%, whereas cellulose contents in stems, roots, and callus tissue were unaffected (Potikha and Delmer, 1995). Other *tbr* phenotypes reported by Potikha and Delmer (1995) included educed trichome density, altered trichome shape and surface appearance, lack of trichome papillae and basal cells, altered stomata shape, and altered patterns of callose deposition.

An additional cell wall-related phenotype was detected when we grew *tbr* mutant seedlings in the dark. Mutant seedlings frequently displayed a marked reduction in hypocotyl length (Fig. 2A), reminiscent of etiolated primary *cesa* mutant seedlings like *prc1-8*, *ixr1-2*, and *rsw1-10* (Fagard et al., 2000; Mouille et al., 2003) and dark-grown wild-type seedlings treated with cellulose synthesis inhibitors like thaxtomin A (Scheible et al., 2003; Bischoff et al., 2009) or dichlobenil (Robert et al., 2004). In addition, young etiolated *tbr* mutant seedlings occasionally showed slight isotropic cell expansion symptoms in the upper part of the hypocotyl (Fig. 2, B and C), a phenotype that was reported previously for thaxtomin A-treated seedlings (Scheible et al., 2003). Such symptoms were never observed in wild-type seedlings (Fig. 2D). These results point to a function of TBR in primary cell wall synthesis in etiolated seedlings. To assess whether this is due to reduced levels of primary wall cellulose, we measured the amount of crystalline cellulose in *tbr* and wild-type hypocotyls (Fig. 2E). We did not detect any differences in cellulose levels between *tbr* and the wild-type control, indicating that alterations in other cell wall polymers may be the cause of the reduced hypocotyl elongation.

Greenhouse-grown *tbr* mutants (i.e. progeny with five backcrosses to ecotype Columbia [Col-0] wild type) also repeatedly displayed a marked growth variation that is unrelated to variation in germination time. The size of *tbr* mutants ranged between wild type like and considerably dwarfed, with the frequency of the latter being less than 10% (Supplemental Fig. S1). Additional visible phenotypes of *tbr* mutants included an approximately 40% reduced stem thickness at the base (0.82 ± 0.12 mm in *tbr* versus 1.47 ± 0.21 mm in the wild type) and reduced leaf size (Supplemental Fig. S1).

Cell Wall Composition of *tbr* Trichomes

To investigate the effects on cell wall composition of the *TBR* gene product, we isolated mature trichomes from *tbr* and wild-type rosette leaves. Cellulose measurements in the trichome preparations revealed an approximately 70% decrease in *tbr* relative to the wild type (Fig. 3), confirming previous results (Potikha and Delmer, 1995). We also analyzed the noncellulosic sugar composition and uronic acid content in trichomes by high-performance anion-exchange chromatography (Fig. 3). Compared with the wild type, *tbr* trichomes displayed a 25% increase of the pectic component GalUA. Similarly, another prominent pectic component, Rha, was increased by approximately 15%. In contrast, the relative Gal and Ara contents were reduced by approximately 15%, while GlcUA, a minor but, for biomineralization processes, important compound found in plant cell walls, was unaltered. Neutral sugars (i.e. Xyl and Fuc), apparent in the side chains of hemicelluloses such as xyloglucans, were increased by around 20% (Fig. 3). A clear separation of Xyl and Man could not be achieved by the high-performance anion-exchange chromatography method used, but additional data obtained from analysis of alditol acetates by gas chromatography-mass spectrometry (data not shown) suggested that the Xyl content was increased in *tbr* mutant trichomes, whereas the Man content was unchanged.

Identification of *TBR*

The morphological changes and the reduction in cellulose in *tbr* mutant trichomes are robust and trans-

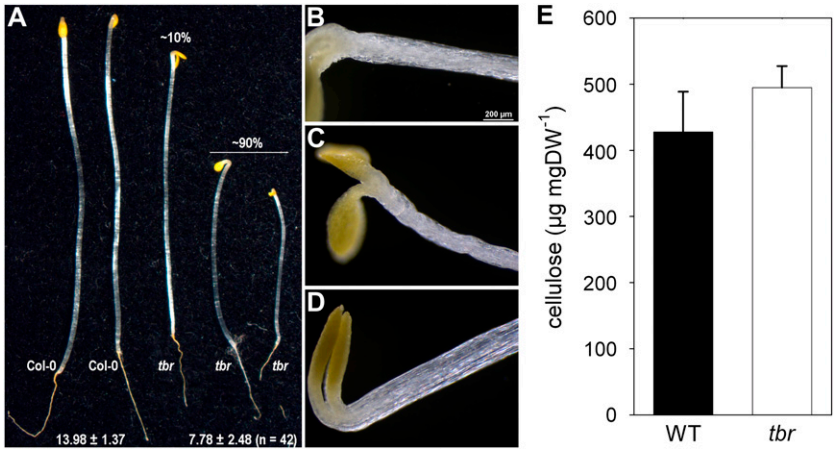

Figure 2. Hypocotyl phenotypes of etiolated *tbr* mutants. A, Aspects of 4-d-old etiolated wild-type and *tbr* mutant seedlings. The length distribution among *tbr* seedlings is indicated by percentage numbers. Numbers at the bottom [13.98 ± 1.37 and 7.78 ± 2.48 (n = 42)] indicate mean values (in millimeters) of hypocotyl length in wild-type and *tbr* populations. B to D, Cell-swelling phenotype occasionally observed at the top of *tbr* mutant hypocotyls (B and C) and the invariant, regular wild-type phenotype (D). E, Crystalline cellulose determination as measured by the Updegraff (1969) protocol. Mean values ± SE (n = 3) are given. DW, Dry weight; WT, wild type.

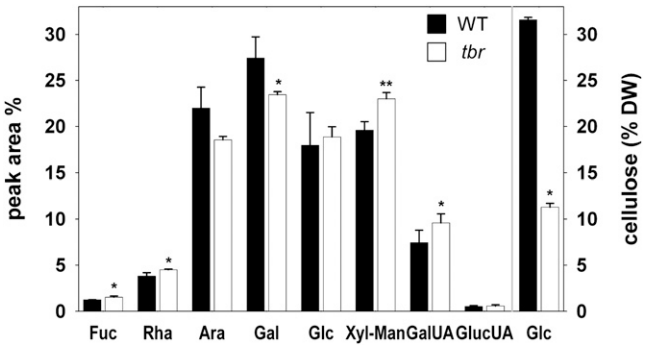

Figure 3. Altered cellulose and noncellulosic sugar composition in *tbr* mutant trichomes. Individual sugars and uronic acids (UA) are expressed as a percentage of the total noncellulosic cell wall sugar. Cellulose-derived Glc (right side) is expressed as a percentage of dry weight (DW). Typical results (means ± SE; $n = 4$) from one of several experiments are shown. Significant changes as deduced from Student's *t* test ($P \leq 0.05$) are marked with asterisks. WT, Wild type.

mitted to the progeny in a pattern typical for recessive mutants (Potikha and Delmer, 1995). Since the genetic lesion in the ethyl methanesulfonate-induced *tbr* mutant was unknown, we identified the *TBR* gene by map-based cloning (Lukowitz et al., 2000) and cosmid complementation (Fig. 4; Supplemental Fig. S2; Supplemental Table S1). This led to the identification of a complementing clone B and an overlapping noncomplementing clone C (Fig. 4; Supplemental Fig. S2). End sequencing of the Arabidopsis genomic sequence integrated in clone B and C revealed that the only *TBR* candidate gene was *AT5G06700*. This gene is completely contained in B, whereas the first two-thirds of the gene is absent in C. Sequencing of *AT5G06700* from *tbr* mutant DNA subsequently revealed a G→A transition in the third exon of the annotated coding region, resulting in replacement of Gly-427 by Glu in the predicted protein (Fig. 4A). A cleaved-amplified polymorphic sequence (CAPS) marker was developed based on the single base change found in *AT5G06700*. Cosegregation of strong trichome birefringence and the heterozygous CAPS genotype was found in the progeny of *tbr* mutants transformed with clone B, as expected (Supplemental Fig. S2D).

To provide further and independent confirmation of the identity of *TBR*, we investigated additional reduction/loss-of-function alleles for *AT5G06700*. To this end, we first tested several T-DNA insertion lines (SALK_134006, SALK_134014, SALK_058509, and SAIL_707_D07) but were unable to (1) identify homozygous mutants by PCR or (2) detect plants with reduced or lacking trichome birefringence. Therefore, we next produced an RNA interference (RNAi) construct to *AT5G06700* and introduced it into the wild type. Many of the resulting RNAi lines displayed considerable or complete loss of trichome birefringence (Fig. 4B). In addition, complementation of the *tbr* mutant was achieved by expression of the annotated *AT5G06700* coding sequence under control of the cauliflower mosaic virus 35S promoter (Supplemental Fig. S3).

TBR and Its Homologs Are Plant-Specific DUF231 Proteins

According to the annotation provided by The Arabidopsis Information Resource (TAIR), *TBR* spans approximately 2.173 kb (from start to stop codon; Fig. 4A), contains five exons, and encodes a 2.207-kb transcript that yields a predicted 608-amino acid 67.9-kD protein with an pI of 9.12. BLASTP and TBLASTN searches with the TBR protein sequence revealed that *TBR* is plant specific and has 45 homologs ($e < 10^{-29}$) in the Arabidopsis genome. We aligned the protein sequences (Supplemental Table S2) and created an unrooted phylogenetic tree (Fig. 5). The proteins cluster into three major branches con-

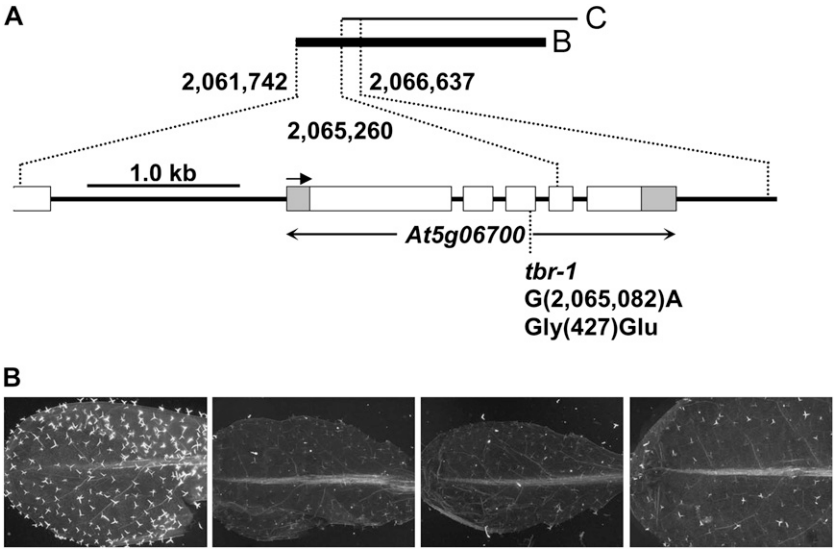

Figure 4. Identification of *TBR*. A, View of the approximately 5-kb region responsible for complementation of the *tbr* phenotype. The structure of the one annotated gene (*AT5G06700*) in that region is given. Exons are depicted as white boxes, and untranslated regions of *AT5G06700* (i.e. *TBR*) are shown as gray boxes. The arrow indicates the direction of transcription. The point mutation in the *tbr-1* allele (G→A) leads to a predicted Gly-to-Glu exchange at position 427 of the encoded protein. B, Knockdown of *TBR* by RNAi (the three photographs to the right show leaves of different RNAi lines) leads to strongly reduced trichome birefringence as compared with the wild type (the photograph to the left).

sistent with previous analyses (Xin et al., 2007), with TBR (AT5G06700) being part of the smallest clade (Fig. 5). Within the family, The Institute for Genomic Research database lists eight pairs of segmental duplicated genes and one triplet that arose through segmental and tandem duplication (highlighted in blue in Fig. 5).

TBR, its duplicated twin *AT3G12060* (*TBL1*), and the closely related *AT1G60790* (*TBL2*) encode the longest annotated proteins in the family (608, 556, and 541 amino acids, respectively), while *AT2G31110* and *AT3G14850* appear to encode the shortest TBL proteins, with 364 and 356 amino acids, respectively (Supplemental Fig. S4A). All of the TBR and TBL homologs harbor a putative transmembrane domain at the N terminus (TMH) and contain a domain of unknown function (DUF231; PFAM 3005; IPR004253) near their C terminus (Supplemental Fig. S4A). The predicted amino acid exchange (Gly-427 → Glu) in the *tbr* mutant introduces a negative charge just in front of the DUF231 domain (asterisk in Supplemental Fig. S4B). This Gly residue is conserved in TBR homologs from other plant species (Supplemental Fig. S4B) as well as 26 of the Arabidopsis TBLs (Supplemental Table S2). Three additional Arabidopsis TBLs have Ala and the residual 16 have an aromatic amino acid (Tyr, Trp, or Phe) in this position.

Furthermore, the 46 proteins contain another plant-specific region, typically 87 to 89 residues long, that has not been recognized previously and that we termed the TBL domain (Supplemental Fig. S4). Thirteen amino acids in this domain, including five unequally spaced Cys residues, two Trp residues, and a Gly-Asp-Ser (GDS) signature, are fully conserved among the 46 family members. In addition, similar amino acids are found in another 25 positions of the TBL domains (Supplemental Fig. S4B; Supplemental Table S2). The GDS signature is followed by a Leu in over half of the proteins (24 proteins) or by a similar nonaromatic, aliphatic amino acid like Ile, Val, or Met, which in turn is preceded by several hydrophobic amino acids. GDS in the same amino acid context (i.e.

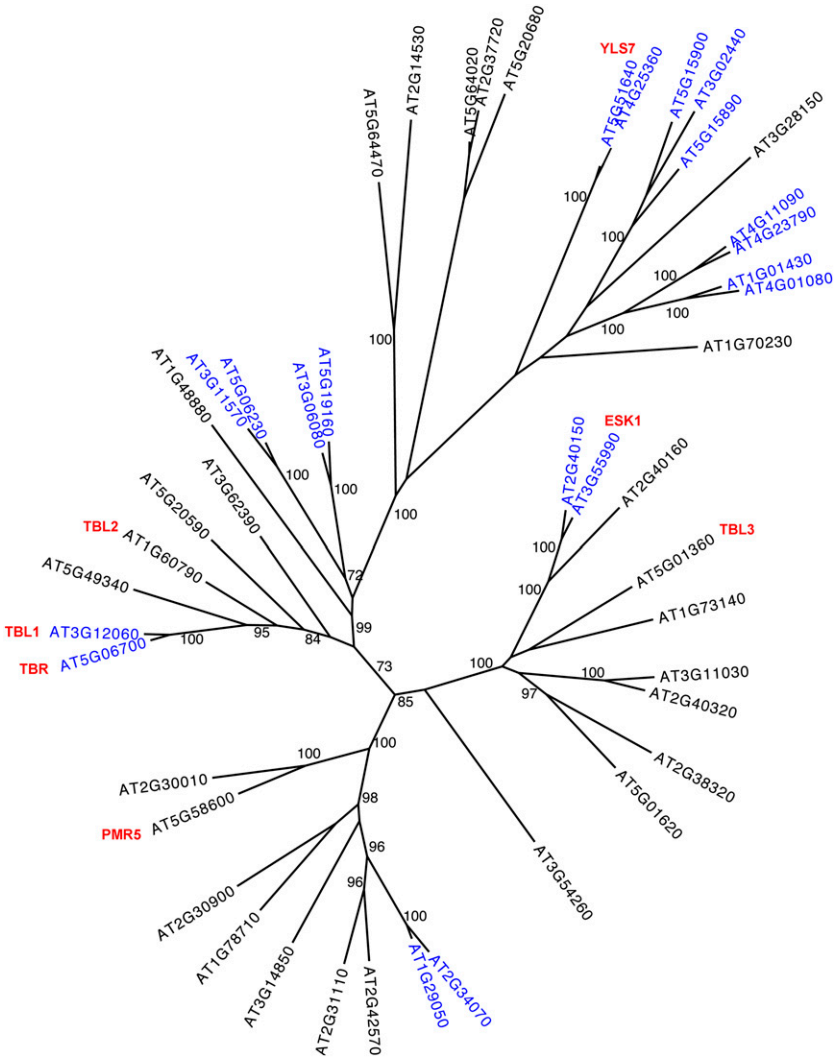

Figure 5. Unrooted, bootstrapped tree of the *TBL* gene family in Arabidopsis. MAFFT (version 5) was used to create an alignment of the protein sequences available at TAIR. Highly variable, gapped N-terminal regions were removed, and a maximum likelihood phylogeny was generated with RAxML model PROTCATWAG (Stamatakis, 2006) and bootstrapped (n = 1,000 trials) to generate the final tree. Bootstrap values greater than 70 are shown. Segmental/tandem gene pairs are highlighted in blue, and genes mentioned in the text are shown in red.

GDSL) has previously been found to be a conserved motif in some esterases/lipases (Upton and Buckley, 1995; Akoh et al., 2004).

Within the 150- to 180-residue-long DUF231 domain, we detected another 13 residues with absolute identity (including another three Cys, three His, and two Trp residues) in all 46 proteins and 27 residues with conserved similarity (Supplemental Fig. S4B; Supplemental Table S2). There is a remarkable stretch of highly conserved amino acids toward the end of the DUF231 domain, including a DxxH motif (Supplemental Fig. S4B; Supplemental Table S2), which is also found in the same class of GDSL motif-containing esterases/lipases. Interestingly, the Asp and His residues in the DxxH motif together with the Ser residue in the distant GDS motif were determined to form the catalytic triad in the 2.5-Å crystal structure of a fungal rhamnogalacturonan acetylesterase (Mølgaard and Larsen, 2004).

TBR/TBLs have highly similar DUF231 protein homologs in other plant species. Within the C-terminal part starting with the TBL domain, TBR, for example, shares 77% identity (90% similarity) with grapevine (*Vitis vinifera*) protein CAO23412, 69% identity (82% similarity) with rice (*Oryza sativa*) lustrin A-like protein BAD35858 (Os06g0207500), and 61% identity (80% similarity) with *Medicago truncatula* protein ABE91344 (Supplemental Fig. S4B).

Expression Pattern of *TBR*

To investigate where the *TBR* gene is active, we created promoter:*GUS* gene reporter lines. When expressed under the control of a 1.6-kb sequence upstream of the annotated start codon (which includes the 140-bp annotated 5′ untranslated region), GUS activity in young plantlets was prominent in leaf and stem trichomes (Fig. 6, A–C). However, similar GUS constructs for the close *TBR* homologs *AT3G12060* (*TBL1*) and *AT1G60790* (*TBL2*) showed that these genes were not active in trichomes (Fig. 6, D and E). Interestingly, the *TBL1* coding sequence expressed under control of the *TBR* promoter complemented the trichome birefringence phenotype of *tbr* mutants (data not shown). These results suggest that TBL1 is functionally equivalent to TBR but may work in different tissues or cell types.

In 3-week-old *TBR*:*GUS* gene reporter plants, GUS activity was mainly associated with the leaf vasculature and was also present in younger expanding/maturating rosette leaves (Fig. 6F) as well as rapidly growing parts of the root (e.g. lateral root tips; data not shown). In 4-week-old plants, the signal persisted in the vasculature and trichomes and was also strong in rapidly expanding, fortifying inflorescence stems (Fig. 6G), where primary and secondary wall cellulose is deposited. With increasing age and organ maturation, GUS activity continuously decreased (Fig. 6H) until it was hardly detectable in 6-week-old plants (Fig. 6I). This expression pattern is in agreement with the developmental AtGenExpress ATH1 gene chip data (Schmid et al., 2005; for visualization, see http://www.bar.utoronto.ca/efp) and is also consistent with the one expected for a component required during cellulose deposition.

Coexpression of *TBR* and *TBL*s with *CESA* and Other Cell Wall Genes

The strong reduction in crystalline cellulose in *tbr* trichomes (Potikha and Delmer, 1995) led us to inves-

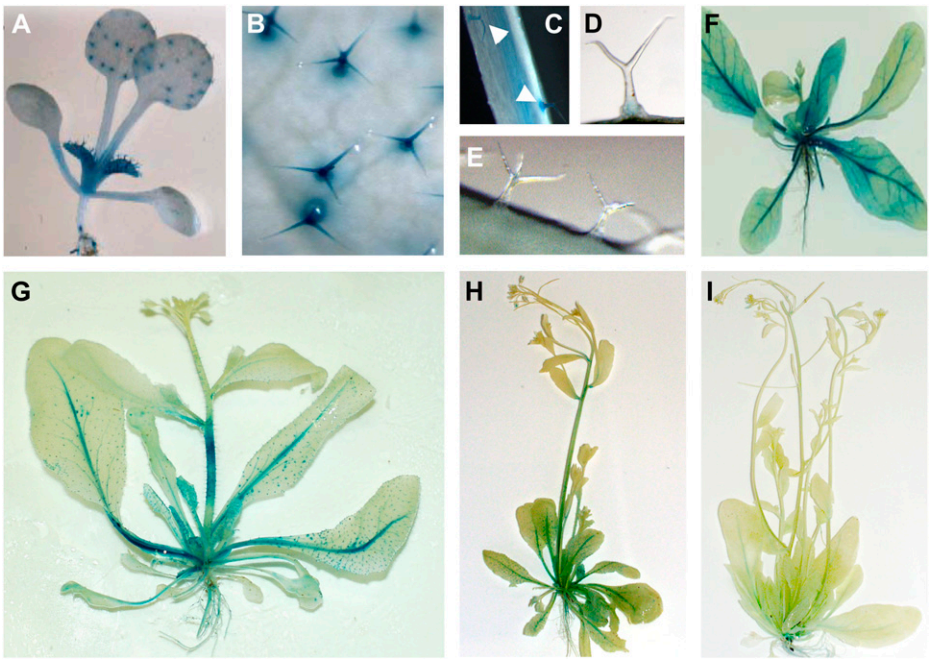

Figure 6. GUS expression of *TBR*. A, Staining of a 9-d-old seedling transformed with *GUS* driven by the *TBR* promoter. B, Magnified view of stained leaf trichomes of a 9-d-old seedling. C to E, Staining of stem trichomes of seedlings transformed with *TBR*:*GUS* (C), *TBL1*:*GUS* (D), or *TBL2*:*GUS* (E). F to I, Typical staining of 3-week-old (F), 4-week-old (G), 5-week-old (H), and 6-week-old (I) *TBR*:*GUS* transgenic plants.

tigate whether the gene is coexpressed with *CESA* genes. Analyses using the GeneCAT coexpression tool (http://genecat.mpg.de; Mutwil et al., 2008) revealed that *CESA5*, *CESA6*, and *CESA3* rank at positions 2, 6, and 12 on the list of genes coexpressed with *TBR* (Supplemental Table S3). We also found the endochitinase *ELP/POM/CTL1* (*AT1G05850*) and the glycophosphatidyl inositol-anchored protein-encoding *COBRA* gene (*AT5G60920*) on this list. These genes are well-known components for primary wall cellulose production (Hauser et al., 1995; Schindelman et al., 2001; Zhong et al., 2002). Similar results were also obtained using other coexpression tools, including ATTED-II (Obayashi et al., 2009) and AraGenNet (Mutwil et al., 2010). Vice versa, *TBR* also appears in the list of coexpressed genes when primary *CESA* genes are used as bait (data not shown; Persson et al., 2005).

To see if other members of the family also may be transcriptionally coordinated with cellulose-related processes, we extended the analysis to include the additional 35 DUF231 family members represented on ATH1 gene chips. Interestingly, the *TBL* gene *AT5G01360* was tightly coexpressed with the secondary *CESA* genes; conversely, the analysis of genes coexpressed with *AT5G01360* in GeneCAT revealed many of the known or suspected genes important for secondary wall cellulose synthesis (Brown et al., 2005), including all three secondary *CESA* genes, *IRX8*, *IRX9*, *IRX12*, and *COBL4* (Supplemental Table S3).

Finally, several other DUF231 family members, including *AT1G78710*, *AT2G37720*, *AT2G40160*, *AT3G28150*, *AT3G62390*, *AT5G01620*, *AT5G15890*, and *AT5G58600*, displayed remarkable coexpression with other cell wall-related genes, like cellulose synthase-like, endo-1,4-β-glucanase, xyloglucan:xyloglucosyl transferase, laccase, polygalacturonase, and pectinesterase genes (http://genecat.mpg.de). Taken together, the coexpression analyses suggest that, besides *TBR*, at least *AT5G01360* and possibly several other members of the plant-specific TBL/DUF231 domain gene family might have a function in cell wall biology.

Isolation and Phenotypic Characterization of *tbl3* Mutants

To investigate the potential involvement of *AT5G01360/TBL3* in cellulose/cell wall synthesis, we obtained seeds from a corresponding T-DNA insertion line (SALK_065959) available through the European Arabidopsis Stock Centre. Homozygous mutant plants were identified by PCR screening of genomic DNA samples and were further characterized for expression of *AT5G01360* (subsequently named *TBL3*) at the cDNA level. No PCR amplification was possible from mutant cDNA with primers spanning the T-DNA insertion site (Supplemental Fig. S5, A and B), and quantitative real-time PCR revealed that the cDNA template corresponding to the last exon of *AT5G01360* was more than 1,000-fold less abundant in the mutant compared with the wild-type cDNA pool (Supplemental Fig. S5, A and C). These results suggest that the isolated homozygous mutant is a null.

Growth analysis revealed that the homozygous mutant progeny displayed a variety of growth phenotypes, ranging from mild to severe reductions in inflorescence stem elongation (Supplemental Fig. S6), whereas rosette leaf or root growth was only mildly affected (Supplemental Fig. S6; data not shown). The variation in growth and stem size is similar to what was observed for the *tbr* mutants (Supplemental Fig. S1). However, *TBR* gene expression was not changed in the *tbl3* mutants (data not shown). The *tbl3* mutants also frequently displayed significantly (10%–20%) reduced stem diameter (data not shown), as found for *tbr* mutants and for other secondary wall mutants (Turner and Somerville, 1997). To corroborate the mutant phenotype, we also produced gene-specific RNAi lines for *AT5G01360* and found the *tbl3* growth phenotypes recapitulated in these (data not shown). These results suggest that *TBL3* is required for normal stem development in Arabidopsis.

Biochemical analysis of *tbl3* T-DNA mutant stems revealed a 15% to 20% reduction in cellulose content independent of stem age (Fig. 7A). These data were reproduced using the *tbl3* RNAi lines (Fig. 7A). We also detected changes in the noncellulosic carbohydrate composition in stem material sampled 20 d after bolting (Fig. 7B). In agreement with previous studies, wild-type stems showed a high Xyl content characteristic of secondary cell walls (Turner and Somerville, 1997; Brown et al., 2005). Cell wall material from *tbl3* mutant stems displayed a 20% relative reduction in Xyl content and strong relative increases in Ara, Gal, Rha, and Fuc as well as uronic acids (Fig. 7B). These changes resemble the sugar compositions measured in

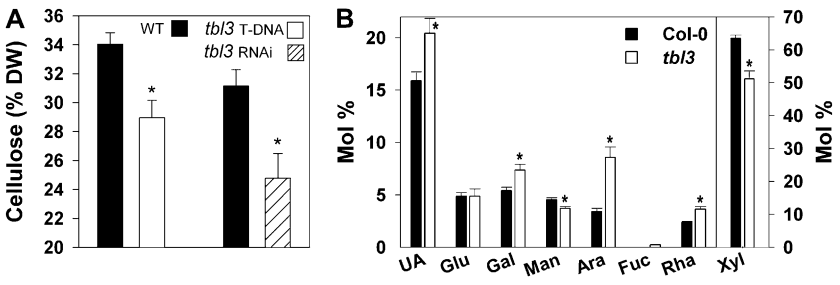

Figure 7. Biochemical cell wall phenotypes of *tbl3* T-DNA mutants. A, Cellulose-derived Glc is expressed as percentage of dry weight (DW) and shows the typical result from one of several experiments (means ± SE; $n = 5$). B, Individual sugars and uronic acids (UA) of wild-type and *tbl3* stems are expressed as percentage of the total noncellulosic cell wall sugar (means ± SE; $n = 4$). Significant changes as deduced from Student's *t* test ($P \leq 0.05$) are marked with asterisks.

stems of *irx7* and *irx8* mutants and of mutants in other genes coexpressed with secondary *CESA*s (Brown et al., 2005; Persson et al., 2007). Finally, stem sections were cut from the base of the mature inflorescence stem to investigate xylem morphology of *tbl3* mutant and the wild type. The xylem vessels of *tbl3* mutants were indistinguishable from wild-type vessels displaying open xylem elements with relatively round shape (data not shown). These data suggest that while the constituents for several important secondary wall polymers were decreased in *tbl3*, the integrity of the wall still is sufficient for normal xylem morphology.

Additional Hypocotyl Phenotypes of *tbr* and *tbl3*

To determine possible structural changes in the cell walls of *tbr* hypocotyls, we performed Fourier transform infrared (FTIR) microspectroscopy (Fig. 8A). This analysis revealed, according to Student's *t* test, significant changes at wave number 1,168 cm^{-1} and also at wave number 1,774 cm^{-1}, which most likely correspond to decreases of ester linkages, presumably of methyl-esterified pectins (Sene et al., 1994; Mouille et al., 2003). The peak at 1,546 cm^{-1} may represent changes in not further specified cell wall proteins. These results indicate that the *tbr* hypocotyls are not holding lower levels of cellulose (Fig. 2E) but that there may be structural changes in the cell wall framework involving esterified pectins. In agreement with this observation, a significantly elevated pectin methylesterase (PME) activity was detected in *tbr* protein extracts derived from etiolated seedlings (Fig. 8B).

In contrast to *tbr* (Fig. 2), etiolated *tbl3* seedlings did not show a significant reduction in hypocotyl length (data not shown). The level of crystalline cellulose in these hypocotyls tended to be slightly increased on a dry weight basis, and FTIR analysis revealed similar changes in cell wall structures of etiolated *tbl3* hypocotyls as seen for *tbr* (Fig. 8A). We found significant changes at wave numbers 852, 917, 933, and 1,191 cm^{-1} and at wave numbers 1,762, 1,731, and 1,712 cm^{-1} (Fig. 8A), indicating structural changes of cellulose and esterified pectins in *tbl3* compared with wild-type seedlings. In addition and similar to *tbr*, PME activity was significantly increased in *tbl3* (Fig. 8B). These data suggest that the *tbr* and *tbl3* seedling hypocotyls hold lower levels of methylesterified pectins due to enhanced PME activities.

DISCUSSION

In this study, we applied forward and reverse genetic approaches to identify two members of the undescribed DUF231 gene family, *TBR* (*AT5G06700*) and *TBL3* (*AT5G01360*), as novel components contributing to secondary wall cellulose synthesis in higher plants. The *tbr* mutant was previously reported as a mutant that lacks crystalline cellulose in trichomes and to lesser extent also in the vasculature (Potikha and Delmer, 1995). The involvement of TBR in cellulose synthesis is underpinned by the expression pattern of the gene. *TBR* displays extraordinary coexpression with primary *CESA* genes, such as *CESA3*, *CESA5*, or *CESA6*, while coexpression with secondary *CESA* genes is inconspicuous. Several genes coexpressed with the primary and secondary *CESA* genes were previously shown to be associated with primary and secondary wall cellulose production, respectively (see introduction and "Results"). The expression patterns obtained from the microarray data sets were mirrored in the *TBR* promoter:GUS staining patterns, corroborating that *TBR* is similarly expressed as the primary wall *CESA* genes. Considering the substantial reduction in trichome-associated crystalline cellulose levels in *tbr*, it is perhaps surprising that no decrease in primary wall cellulose levels were observed. However, it is possible that other TBR-related gene products may functionally compensate for the loss of TBR in these

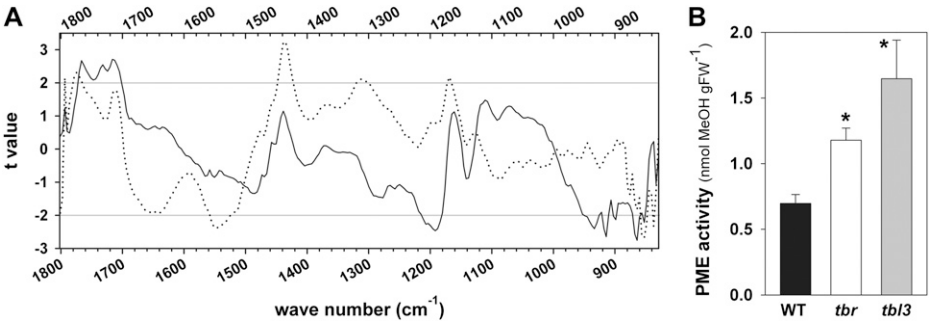

Figure 8. FTIR spectra and PME activity in *tbr* and *tbl3* mutants. A, FTIR spectrum from 4-d-old, dark-grown *tbr* (dotted line) and *tbl3* (solid line) mutant hypocotyls. Student's *t* test values for the comparison between the wild type and *tbr* or *tbl3* (*x* axis) are plotted against the wave numbers (*y* axis). Horizontal gray lines refer to the significance threshold ($P = 0.95$). Several highly significant maxima can be assigned to pectin ester linkages and alterations in cell wall crystallinity. B, Measurement of PME activity isolated from etiolated seedlings. The mean values of PME activity are expressed as release of methanol in nmol g^{-1} fresh weight (FW) derived from wild-type (WT), *tbr*, and *tbl3* seedlings. Mean values ± SE are shown ($n = 5$). Significant changes ($P \leq 0.01$) as deduced from Student's *t* test are marked with asterisks.

tissues. In support of such scenario, *TBL1* could rescue the trichome birefringence phenotype when expressed under the control of the *TBR* promoter.

We showed that the reduction in cellulose content in *tbr* trichomes was accompanied by an increased amount of pectic compounds (i.e. GalUAs), whereas the relative Gal and Ara contents were reduced by approximately 15%. These results imply increased amounts of HG and decreased abundance of the Gal- and Ara-containing side chains of the pectin rhamnogalacturonan I in the mutant. The amount of GlcUA remained stable in trichomes, in turn. This result confirms that the changes in uronic acids are associated with pectic structures and rules out the idea that loss of trichome birefringence is a result of reduced uronic acid-dependent biomineralization/crystallization. The amount of Xyl-Man was increased, indicating elevated amounts of xyloglucans. Since the effects on pectin/xyloglucan content, and/or modification, were significant, we propose that *tbr* directly interferes with cellulose biosynthesis in trichomes and directly or indirectly influences pectin composition in this organ. In support of this, several mutants deficient in cellulose production display increased levels of pectins, most likely homogalacturonans (His et al., 2001).

tbr hypocotyls contained wild-type levels of primary wall cellulose, less methylesterified pectins, and hold modified cell wall structures, as assessed by FTIR analysis. In addition, results of the PME assay confirm that the lower degree of pectin methylesterification comes along with a higher methylesterase activity in *tbr* compared with wild-type seedlings. Many primary cell wall mutants (e.g. *prc1-1*, *rsw1-10*, *kor1-1*, and *kob1-1*) have less crystalline cellulose and short hypocotyls (Desnos et al., 1996; Arioli et al., 1998; Nicol et al., 1998; Fagard et al., 2000; Pagant et al., 2002). However, dwarfed hypocotyls are not necessarily linked to the level of crystalline cellulose but can also result from altered levels of methylesterified pectins (Derbyshire et al., 2007). In addition, it is interesting that the *tbr* hypocotyl phenotypes described partially resemble the mutant *quasimodo2* (*qua2*), affecting a putative pectin methyltransferase. *qua2* has higher levels of crystalline cellulose, a shorter hypocotyl, as well as altered pectin composition (Mouille et al., 2003, 2007). Our results suggest that *TBR*, besides its role in secondary wall cellulose deposition in trichomes, is involved in pectin modifications in etiolated hypocotyls, a tissue mainly containing primary wall cellulose. Alternatively, the changes described could reflect a feedback loop from secondary to primary cell wall biosynthesis, as has been described for *mur10* (Bosca et al., 2006). However, *TBR* has a largely nonredundant/critical biological function in trichomes, as suggested by the missing trichome expression of its close homologs (Fig. 6, D and E). In this context, it is interesting (1) that Arabidopsis trichomes do not appear to express secondary *CESA* genes (*CESA4*, *CESA7*, and *CESA8*) while primary *CESA* genes (*CESA1*, *CESA3*, *CESA5*, and *CESA6*) and *KORRIGAN* are expressed (Jakoby et al., 2008; Marks et al., 2008), and (2) that the Arabidopsis trichome cell wall contains polysaccharides that are more like those of typical primary walls (Marks et al., 2008). This may suggest that the "secondary wall" crystalline cellulose deposited in trichomes is a product of the primary CESA complex. Alternatively, the secondary CESA complex may be recruited from other cell types, such as neighboring trichome companion or basal cells. However, both interpretations seem to be rejected by the observation that *irx3* (*cesa7*) mutants as well as primary *cesa* mutants (*cesa3*, *cesa2*, *cesa5*, *cesa6*, *cesa2/cesa5*, and *cesa2/cesa6*) display wild-type-like trichome birefringence (V. Bischoff, S. Nita, and W. Scheible, unpublished data). Another possibility would be that cellulose synthase-like proteins synthesize cellulose in trichomes, similar to the situation described for pollen tubes of *Nicotiana alata* (Doblin et al., 2001).

The second TBL/DUF231 domain gene family member that we functionally implicated in secondary cell wall and cellulose synthesis is *TBL3* (*AT5G01360*). This gene was strongly coexpressed with *CESA4*, *CESA7*, and *CESA8*, and analysis of a T-DNA insertion null allele and RNAi lines confirmed its function in secondary cell wall cellulose deposition. The T-DNA mutants have shorter and weaker stems at high frequency, contained significantly less cellulose in the inflorescence stems, and displayed a cell wall monosaccharide pattern that highly resembles those of several *irx* mutants (Brown et al., 2005). *tbl3* stems appear to be enriched in pectin, as judged from increased levels of uronic acids, Ara, Gal, and Rha. While Xyl levels decreased by approximately 20%, this neutral sugar pattern is reminiscent of those found in *irx7*, *irx8*, and *irx9* mutants (Brown et al., 2005). The irregular xylem structure is a known criterion for mutants involved in secondary wall cellulose biosynthesis (Turner and Somerville, 1997). However, the reduction of cellulose and/or the structural changes in the secondary cell wall of *tbl3* were not sufficient to yield an irregular xylem phenotype with collapsed xylem vessels (data not shown). This is in agreement with several other mutants notably involved in secondary wall cellulose biosynthesis. Some of the latter showed normal or modestly disturbed xylem vessels (Brown et al., 2005, 2009; Persson et al., 2005), while others developed the irregular xylem phenotype only in a double *irx* background (Brown et al., 2009). Additional analyses showed that etiolated *tbl3* hypocotyls displayed wild-type-like phenotypes but, as seen for *tbr* hypocotyls, had slightly elevated crystalline cellulose levels and significantly reduced amounts of methylesterified pectins. Along with the PME assay showing higher PME activity in *tbl3*, our results suggest that *TBL3*, similar to *TBR*, is involved in secondary wall cellulose biosynthesis in specific tissues and also has an influence on the pectic structures in tissue containing mainly primary cell wall. A role of *AT5G01360* in secondary cell wall biosynthesis was previously suggested, as it turned up as a member of a

core xylem-specific gene set resulting from global comparative transcriptome analysis (Ko et al., 2006).

What might be the biochemical functions of the plant-specific DUF231 domain genes? One report (Yoshida et al., 2001) describes *YLS7* (*AT5G51640*) as highly expressed in senescent leaves, but beyond this the gene remained anonymous. Another member of the gene family (*ESK1*; *AT3G55990*) was found to act as a negative regulator of cold acclimation, as mutations in the *ESK1* gene provide strong freezing tolerance (Xin et al., 2007). In a third report, it was noted that a null mutation in the *PMR5* gene (i.e. *AT5G58600*) rendered Arabidopsis resistant to powdery mildew species and that, based on cell wall and FTIR analyses, *pmr5* cell walls were enriched in pectin and displayed a reduced degree of pectin methylesterifiation relative to wild-type cell walls, suggesting that the gene affects pectin composition (Vogel et al., 2004). This observation is in line with our results, as we also noted changes in pectin composition in various tissues of *tbr* and *tbl3*. Although the alterations in pectin composition in *tbr* trichomes and *tbl3* stems seem to be due to compensatory effects following the reduction in cellulose levels, our results from etiolated *tbr* and *tbl3* hypocotyls suggest a more direct impact of these gene products on pectin modification. FTIR analysis revealed less esterified pectins, and this could be confirmed by an elevated PME activity. These results indicate that at least some DUF231 gene family members, including PMR5, TBR, and TBL3, are required to maintain higher pectin methylesterification states, for example by inhibiting PME activity, rather than being PMEs by themselves, as might be deduced from the conserved GDSL and DxxH motifs known from some esterases (see "Results").

Whatever the biochemical function of the proteins, loss of TBR or TBL3 appears to increase PME activity, reduce pectin esterification, and decrease cellulose deposition in trichomes and stems, respectively. There is existing evidence indicating that correct modifications of noncellulosic cell wall polysaccharides are important for growth of cells undergoing secondary wall thickening, the synthesis of secondary wall cellulose, and secondary wall integrity. For example, the dwarfed Arabidopsis *irx8/gaut12* mutant is deficient in GX and HG (Persson et al., 2007), has alterations of the glycosyl sequence at the GX reducing end (Peña et al., 2007), and shows a significant reduction in secondary cell wall thickness and cellulose content (Persson et al., 2007). The degree of pectin methylesterification can limit cell growth and hypocotyl elongation in Arabidopsis, as shown by ectopic expression of a fungal PME (Derbyshire et al., 2007). Similarly, PME prevents correct growth of developing wood cells/fibers in poplar (*Populus* species; Siedlecka et al., 2008), suggesting that proper pectin esterification is likely to be essential for xylem development and lignification (Pelloux et al., 2007). Furthermore, there is evidence for potent binding of pectins, which are enriched in neutral side chains, to cellulose (Zykwinska et al., 2005), thus leading to the assumption that pectin-cellulose interactions are significant for cell wall assembly and normal cellulose deposition during primary and secondary cell wall formation. In tobacco leaf explants, oligogalacturonides derived from esterified HG were shown to stimulate cellulose deposition and cell wall thickening (Altamura et al., 1998), and such oligogalacturonides were also shown to elicit the production of hydrogen peroxide (H_2O_2; Legendre et al., 1993; Svalheim and Robertsen, 1993), probably via induction of small Rac-type GTPases, which activate H_2O_2-producing plasma membrane NADPH oxidases (Keller et al., 1998; Potikha et al., 1999; Wong et al., 2007). In this respect, it should be noted that the plasma membrane-localized small GTPase AtRAC2/ROP7 (*AT5G45970*) is specifically induced during later stages of xylem differentiation in Arabidopsis (Brembu et al., 2005), and strong coexpression with *TBL3* was detected in our study (Supplemental Table S3). Constant production of low levels of H_2O_2 stimulates the onset of secondary wall cellulose synthesis and secondary wall differentiation, as shown in cotton fiber cells (Potikha et al., 1999; Karlsson et al., 2005; Hovav et al., 2008), which from the botanical point of view represent seed trichomes. It is tempting, therefore, to speculate that (1) TBR and/or TBL3 function in maintaining HG esterification, as suggested by our results, and that (2) this is required for triggering secondary wall cellulose synthesis in a manner similar to the suite of events outlined above. Therefore, the esterification state of pectic polymers might influence the synthesis and deposition of cellulose in plants.

MATERIALS AND METHODS

Plant Materials and Growth Conditions

Arabidopsis (*Arabidopsis thaliana*) plants were grown in environmental chambers (120 μE, 16 h of light/8 h of dark, 60% relative humidity, 20°C) or in the greenhouses of the Max Planck Institute of Molecular Plant Physiology (150 μE, 12–14 h of light, approximately 70% relative humidity, 20°C–22°C) on a commercial Arabidopsis substrate (Stender). Etiolated seedlings were grown on vertical agar plates (0.7% [w/v] agar, half-strength Murashige and Skoog medium supplemented with 0.5% [w/v] Suc) wrapped in aluminum foil. Arabidopsis wild-type (Col-0) and *tbr* mutant seeds were obtained from an in-house collection. The *tbl3* T-DNA insertion line SALK_065959 was obtained from the European Arabidopsis Stock Centre.

Positional Cloning of the *TBR* Locus

See Supplemental Protocol S1.

Cell Wall Analyses and PME Activity Assay

See Supplemental Protocols S2 and S3.

Analysis of Trichome Birefringence

Trichome birefringence of old rosette leaves was analyzed by incubation in methanol for 20 min followed by discoloration for 1 h in boiling 85% lactic acid and rinsing with water (three times). The leaves were then observed with a stereomicroscope (Leica MZ 12.5) equipped with a polarizer.

Stem Cross-Sections

The 50-μm cross-sections were cut with a vibratome (Leica). Sections were stained with 0.1% toluidine blue (analysis of irregular xylem structures) and observed with a stereomicroscope (Olympus BX41 and Leica MZ 125).

FTIR Microspectrometry

Four-day-old seedlings were squashed between two barium fluoride windows and rinsed abundantly with distilled water for 2 min before drying at 37°C for 20 min. For each mutant, 20 spectra were collected from individual hypocotyls of seedlings from four independent cultures (five seedlings from each culture), as described by Mouille et al. (2003). Normalization of the data and statistical analyses were performed as described by Mouille et al. (2003). Normalization of the data set and statistical analyses were performed using the statistical language R version 2.6. (R Development Core Team, 2006). To normalize the spectra, the baseline, estimated using a linear regression involving 10 points at each end of the spectrum, was subtracted from each absorbance value, and the area was set to 1 by dividing each absorbance value by the sum of all absorbance values. To determine the difference of the composition and the structure between mutants and the wild type, Student's *t* test was performed.

RNAi Constructs for *TBR* and *TBL3*

A 381-bp *TBR*-specific PCR fragment was amplified using primers 5′-CACCAACCACTCGTCACGCGCC-3′ and 5′-GGTTTGGTTGAAGTGACATTGGG-3′, subcloned into pENTR/SD/D-TOPO (Invitrogen), and recombined into pK7GWIWG2(II) (Karimi et al., 2002). A 177-bp *TBL3*-specific PCR fragment was amplified with primers 5′-CACCAATTACCAGATTTGCCACTATGAGC-3′ and 5′-TTGAAGAAAGATGAAGACGAAGAGG-3′ and shuttled into pK7GWIWG2(II) with the same strategy. The constructs were transferred into Col-0 plants by *Agrobacterium tumefaciens*-mediated transformation (Clough and Bent, 1998), and T1 transformants were selected on kanamycin and scored for trichome birefringence as described above.

Promoter:*GUS* Constructs and GUS Staining

To obtain a *TBR* promoter:*GUS* gene fusion construct, a PCR product was amplified from genomic DNA of Arabidopsis wild-type Col-0 using PfuTurbo polymerase (Stratagene) and primers 5′-CAAT*GTCGAC*GGAAGATGAGTTGGACAATGC-3′ and 5′-CAAT*GGATCC*GCATATACTTAACGGCGTCTG-3′. The 1.64-kb *Bam*HI/*Sal*I promoter fragment was subsequently fused to the GUS gene in vector pBI101.1 (Clontech); after sequence verification, the recombinant vector was introduced into Arabidopsis wild-type Col-0 via *A. tumefaciens* (GV3101) according to Clough and Bent (1998). Detection of GUS activity was performed according to Jefferson et al. (1987) by incubation in staining buffer at 37°C overnight. Promoter:*GUS* lines for the close *TBR* homologs *AT3G12060* (*TBL1*) and *AT1G60790* (*TBL2*) were produced likewise using primers 5′-CAAT*GTCGAC*TTTCGGAGTTTCTAGTCTGGA-3′ and 5′-CAAT*GGATCC*TTCAGGCAATGCGTAATCTAT-3′ and primers 5′-CAAT*GTCGAC*CCATTTGTATCAATCTCCCCC-3′ and 5′-CAATC*CCGGG*AATGAAGCACACGGAAAGTGA-3′, respectively.

Molecular Analysis of *tbl3* Mutants

A T-DNA insertion line (SALK_065959) for *TBL3* (*AT5G01360*) was obtained from the European Arabidopsis Stock Centre. Plant DNA was extracted as described previously (Lukowitz et al., 2000). Mutant lines were confirmed for T-DNA insertion using spanning primers LP (5′-GTATGAAAAACGGACAGCCAGAAACT-3′) and RP (5′-TCCGAAAGAACCCCACAGAGC-3′; designed on http://signal.salk.edu/tdnaprimers.html) and a primer from the left T-DNA border, LBc1 (5′-CCGCAATGTGTTATTAAGTTG-3′). Primer combinations LBC1/LP and LP/RP were used. PCR conditions were 96°C for 5 min; 96°C for 30 s, 58°C for 40 s, and 72°C for 1 min; 4°C hold. RNA was isolated from *tbl3* mutant stems using the Plant RNeasy Mini Kit (Qiagen). RNA quality checks, DNase I treatment, and reverse transcription were performed as described previously (Czechowski et al., 2005). PCR with the primers 5′-GTATGAAAAACGGACAGCCAGAAACT-3′ and 5′-TCCGAAAGAACCCCACAGAGC-3′ spanning the insertion site (Supplemental Fig. S5A) was performed on wild-type and *tbl3* cDNA to confirm the absence of a PCR product when using the mutant template (Supplemental Fig. S5B). Quantitative real-time PCR was used to analyze the expression level of *AT5G01360* using an Applied Biosystems HT7900 sequence detection system, SYBR Green reagent (Applied Biosystems), and primers 5′-ATCGCATCGACGCTCACAC-3′ and 5′-TCAGCGGTTAGGATCTTGCC-3′. For further details and subsequent data normalization procedures, see Czechowski et al. (2005).

Sequence Alignment and Phylogenetic Analysis

MAFFT version 5 (Katoh and Toh, 2005) was used to create an alignment of the Arabidopsis DUF231 protein sequences available at TAIR and that of other plant TBR homologs available at the National Center for Biotechnology Information. The alignment was processed with Boxshade 3.21 (http://www.ch.embnet.org) and arranged manually into the final layout (Supplemental Fig. S4B; Supplemental Table S2). Prior to computing a phylogeny, the highly variable and gapped N-terminal region was removed manually, and all columns with 50% or more gaps were removed with the software REAP (Hartmann and Vision, 2008). RAxML version 7 was then used to compute an unrooted maximum likelihood phylogeny from the masked alignment using the PROTCATWAG model (Stamatakis, 2006). The phylogenetic tree was subsequently bootstrapped (n = 1,000 trials) to create the final tree in FigTree version 1.1.2 (http://tree.bio.ed.ac.uk/software/figtree/) as shown in Figure 5.

Coexpression Analysis

Coexpression analyses were performed using the Web-based tool GeneCAT (Mutwil et al., 2008) and ATTED-II (Obayashi et al., 2009).

Sequence data from this article can be found in the Arabidopsis Genome Initiative database under the following locus identifiers: *AT5G06700* (*TBR*), *AT3G12060* (*TBL1*), *AT1G60790* (*TBL2*), and *AT5G01360* (*TBL3*). The mutant *tbr* sequence is available from GenBank (HM120873).

Supplemental Data

The following materials are available in the online version of this article.

Supplemental Figure S1. Growth phenotype of *tbr* mutants.

Supplemental Figure S2. Identification of *TBR* by recombinational mapping and cosmid complementation.

Supplemental Figure S3. Complementation of the *tbr* mutant by 35S::TBR.

Supplemental Figure S4. Structure and sequence alignment of DUF231 domain proteins.

Supplemental Figure S5. Molecular characterization of *tbl3* T-DNA insertion mutants.

Supplemental Figure S6. Growth phenotype of *tbl3* mutants.

Supplemental Table S1. Specifications and primer sequences of mapping markers and the *tbr* CAPS marker.

Supplemental Table S2. Partial alignment of the 46 Arabidopsis DUF231 proteins.

Supplemental Table S3. Genes coexpressed with *TBR* or *TBL3*.

Supplemental Protocol S1. Positional cloning of the *tbr* locus.

Supplemental Protocol S2. Biochemical analyses of *tbr* and *tbl3* cell walls.

Supplemental Protocol S3. PME extraction and activity assay.

ACKNOWLEDGMENTS

We are grateful to Kian Hematy and Gregory Mouille (both INRA), and Eugenia Maximova (Max Planck Institute of Molecular Plant Physiology) for excellent advice and help with respect to microscopy and to Joachim Selbig and Stefanie Hartmann (both University of Potsdam) for help with phylogenetic analysis. We also acknowledge Erwin Grill (Technical University

Munich) for providing the Col-0 cosmid library, CEREON Genomics for supplying information on Col-0/Landsberg *erecta* polymorphisms, and the European Arabidopsis Stock Centre for seeds of the T-DNA insertion line SALK_065959.

Received January 13, 2010; accepted April 12, 2010; published April 13, 2010.

LITERATURE CITED

Akoh CC, Lee GC, Liaw YC, Huang TH, Shaw JF (2004) GDSL family of serine esterases/lipases. Prog Lipid Res **43:** 534–552

Altamura MM, Zaghi D, Salvi G, De Lorenzo G, Bellincampi D (1998) Oligogalacturonides stimulate pericycle cell wall thickening and cell divisions leading to stoma formation in tobacco leaf explants. Planta **204:** 429–436

Arioli T, Peng L, Betzner AS, Burn J, Wittke W, Herth W, Camilleri C, Höfte H, Plazinski J, Birch R, et al (1998) Molecular analysis of cellulose biosynthesis in Arabidopsis. Science **279:** 717–720

Bauer S, Vasu P, Persson S, Mort AJ, Somerville CR (2006) Development and application of a suite of polysaccharide-degrading enzymes for analyzing plant cell walls. Proc Natl Acad Sci USA **103:** 11417–11422

Bischoff V, Cookson SJ, Wu S, Scheible WR (2009) Thaxtomin A affects CESA-complex density, expression of cell wall genes, cell wall composition, and causes ectopic lignification in Arabidopsis thaliana seedlings. J Exp Bot **60:** 955–965

Bosca S, Barton CJ, Taylor NG, Ryden P, Neumetzler L, Pauly M, Roberts K, Seifert GJ (2006) Interactions between MUR10/CesA7-dependent secondary cellulose biosynthesis and primary cell wall structure. Plant Physiol **142:** 1353–1363

Braam J (1999) If walls could talk. Curr Opin Plant Biol **2:** 521–524

Brembu T, Winge P, Bones AM (2005) The small GTPase AtRAC2/ROP7 is specifically expressed during late stages of xylem differentiation in Arabidopsis. J Exp Bot **56:** 2465–2476

Brown DM, Zeef LA, Ellis J, Goodacre R, Turner SR (2005) Identification of novel genes in *Arabidopsis* involved in secondary cell wall formation using expression profiling and reverse genetics. Plant Cell **17:** 2281–2295

Brown DM, Zhang Z, Stephens E, Dupree P, Turner SR (2009) Characterization of IRX10 and IRX10-like reveals an essential role in glucuronoxylan biosynthesis in Arabidopsis. Plant J **57:** 732–746

Burk DH, Liu B, Zhong R, Morrison WH, Ye ZH (2001) A katanin-like protein regulates normal cell wall biosynthesis and cell elongation. Plant Cell **13:** 807–827

Burn JE, Hocart CH, Birch RJ, Cork AC, Williamson RE (2002) Functional analysis of the cellulose synthase genes *CesA1*, *CesA2*, and *CesA3* in Arabidopsis. Plant Physiol **129:** 797–807

Carpita N, McCann M (2000) The cell wall. *In* B Buchanan, W Gruissem, R Jones, eds, Biochemistry and Molecular Biology of Plants. American Society of Plant Physiologists, Rockville, MD, pp 52–108

Carpita NC, Tierney M, Campbell M (2001) Molecular biology of the plant cell wall: searching for the genes that define structure, architecture, and dynamics. Plant Mol Biol **47:** 1–5

Clough SJ, Bent AF (1998) Floral dip: a simplified method for *Agrobacterium*-mediated transformation of *Arabidopsis thaliana*. Plant J **16:** 735–743

Czechowski T, Stitt M, Altmann T, Udvardi MK, Scheible WR (2005) Genome-wide identification and testing of superior reference genes for transcript normalization in Arabidopsis. Plant Physiol **139:** 5–17

Derbyshire P, McCann MC, Roberts K (2007) Restricted cell elongation in Arabidopsis hypocotyls is associated with a reduced average pectin esterification level. BMC Plant Biol **7:** 31

Desnos T, Orbović V, Bellini C, Kronenberger J, Caboche M, Traas J, Höfte H (1996) Procuste1 mutants identify two distinct genetic pathways controlling hypocotyl cell elongation, respectively in dark- and light-grown Arabidopsis seedlings. Development **122:** 683–693

Doblin MS, De Melis L, Newbigin E, Bacic A, Read SM (2001) Pollen tubes of *Nicotiana alata* express two genes from different β-glucan synthase families. Plant Physiol **125:** 2040–2052

Ebringerova A, Heinze T (2000) Naturally occurring xylans: structures, isolation procedures and properties. Macromol Rapid Commun **21:** 542–556

Fagard M, Desnos T, Desprez T, Goubet F, Refregier G, Mouille G, McCann M, Rayon C, Vernhettes S, Höfte H (2000) *PROCUSTE1* encodes a cellulose synthase required for normal cell elongation specifically in roots and dark-grown hypocotyls of *Arabidopsis*. Plant Cell **12:** 2409–2424

Hartmann S, Vision TJ (2008) Using ESTs for phylogenomics: can one accurately infer a phylogenetic tree from a gappy alignment? BMC Evol Biol **8:** 95

Hauser MT, Morikami A, Benfey PN (1995) Conditional root expansion mutants of Arabidopsis. Development **121:** 1237–1252

His I, Driouich A, Nicol F, Jauneau A, Höfte H (2001) Altered pectin composition in primary cell walls of korrigan, a dwarf mutant of Arabidopsis deficient in a membrane-bound endo-1,4-β-glucanase. Planta **212:** 348–358

Hovav R, Udall JA, Chaudhary B, Hovav E, Flagel L, Hu G, Wendel JF (2008) The evolution of spinnable cotton fiber entailed prolonged development and a novel metabolism. PLoS Genet **4:** e25

Hu Y, Zhong R, Morrison WH, Ye ZH (2003) The Arabidopsis RHD3 gene is required for cell wall biosynthesis and actin organization. Planta **217:** 912–921

Jakoby MJ, Falkenhan D, Mader MT, Brininstool G, Wischnitzki E, Platz N, Hudson A, Hülskamp M, Larkin J, Schnittger A (2008) Transcriptional profiling of mature Arabidopsis trichomes reveals that NOECK encodes the MIXTA-like transcriptional regulator MYB106. Plant Physiol **148:** 1583–1602

Jefferson RA, Kavanagh TA, Bevan MW (1987) GUS fusions: beta-glucuronidase as a sensitive and versatile gene fusion marker in higher plants. EMBO J **6:** 3901–3907

Jones DA, Takemoto D (2004) Plant innate immunity: direct and indirect recognition of general and specific pathogen-associated molecules. Curr Opin Immunol **16:** 48–62

Karimi M, Inzé D, Depicker A (2002) GATEWAY vectors for *Agrobacterium*-mediated plant transformation. Trends Plant Sci **7:** 193–195

Karlsson M, Melzer M, Prokhorenko I, Johansson T, Wingsle G (2005) Hydrogen peroxide and expression of hipI-superoxide dismutase are associated with the development of secondary cell walls in *Zinnia elegans*. J Exp Bot **56:** 2085–2093

Katoh K, Toh M (2005) MAFFT version 5: improvement in accuracy of multiple sequence alignment. Nucleic Acids Res **33:** 511–518

Keller T, Damude HG, Werner D, Doerner P, Dixon RA, Lamb C (1998) A plant homolog of the neutrophil NADPH oxidase gp91-phox subunit gene encodes a plasma membrane protein with Ca21-binding motifs. Plant Cell **10:** 255–266

Ko JH, Beers EP, Han KH (2006) Global comparative transcriptome analysis identifies gene network regulating secondary xylem development in *Arabidopsis thaliana*. Mol Genet Genomics **276:** 517–531

Legendre L, Rueter S, Heinstein PF, Low PS (1993) Characterization of the oligogalacturonide-induced oxidative burst in cultured soybean (*Glycine max*) cells. Plant Physiol **102:** 233–240

Lertpiriyapong K, Sung Z (2003) The *elongation defective1* mutant of Arabidopsis is impaired in the gene encoding a serine-rich secreted protein. Plant Mol Biol **53:** 581–595

Lukowitz W, Gillmor CS, Scheible WR (2000) Positional cloning in Arabidopsis: why it feels good to have a genome initiative working for you. Plant Physiol **123:** 795–805

Marks MD, Betancur L, Gilding E, Chen F, Bauer S, Wenger JP, Dixon RA, Haigler CH (2008) A new method for isolating large quantities of Arabidopsis trichomes for transcriptome, cell wall and other types of analyses. Plant J **56:** 483–492

Mølgaard A, Larsen S (2004) Crystal packing in two pH-dependent crystal forms of rhamnogalacturonan acetylesterase. Acta Crystallogr Sect D **60:** 472–478

Mouille G, Ralet MC, Cavelier C, Eland C, Effroy D, Hématy K, McCartney L, Truong HN, Gaudon V, Thibault JF, et al (2007) Homogalacturonan synthesis in Arabidopsis thaliana requires a Golgi-localized protein with a putative methyltransferase domain. Plant J **50:** 605–614

Mouille G, Robin S, Lecomte M, Pagant S, Höfte H (2003) Classification and identification of Arabidopsis cell wall mutants using Fourier-transform infrared (FT-IR) microspectroscopy. Plant J **35:** 393–404

Mutwil M, Obro J, Willats WG, Persson S (2008) GeneCAT: novel Webtools that combine BLAST and co-expression analyses. Nucleic Acids Res **36:** W320–W326

Mutwil M, Usadel B, Schütte M, Loraine A, Ebenhöh O, Persson S (2010) Assembly of an interactive correlation network for the Arabidopsis

genome using a novel heuristic clustering algorithm. Plant Physiol **152:** 29–43

Nicol F, His I, Jauneau A, Vernhettes S, Canut H, Höfte H (1998) A plasma membrane-bound putative endo-1,4-beta-D-glucanase is required for normal wall assembly and cell elongation in Arabidopsis. EMBO J **17:** 5563–5576

Obayashi T, Hayashi S, Saeki M, Ohta H, Kinoshita K (2009) ATTED-II provides coexpressed gene networks for Arabidopsis. Nucleic Acids Res **37:** D987–D991

Pagant S, Bichet A, Sugimoto K, Lerouxel O, Desprez T, McCann M, Lerouge P, Vernhettes S, Höfte H (2002) *KOBITO1* encodes a novel plasma membrane protein necessary for normal synthesis of cellulose during cell expansion in *Arabidopsis*. Plant Cell **14:** 2001–2013

Pear JR, Kawagoe Y, Schreckengost WE, Delmer DP, Stalker DM (1996) Higher plants contain homologs of the bacterial *celA* genes encoding the catalytic subunit of cellulose synthase. Proc Natl Acad Sci USA **93:** 12637–12642

Pelloux J, Rustérucci C, Mellerowicz EJ (2007) New insights into pectin methylesterase structure and function. Trends Plant Sci **12:** 267–277

Peña MJ, Zhong R, Zhou GK, Richardson EA, O'Neill MA, Darvill AG, York WS, Ye ZH (2007) *Arabidopsis irregular xylem8* and *irregular xylem9*: implications for the complexity of glucuronoxylan biosynthesis. Plant Cell **19:** 549–563

Persson S, Caffall KH, Freshour G, Hilley MT, Bauer S, Poindexter P, Hahn MG, Mohnen D, Somerville C (2007) The *Arabidopsis irregular xylem8* mutant is deficient in glucuronoxylan and homogalacturonan, which are essential for secondary cell wall integrity. Plant Cell **19:** 237–255

Persson S, Wei H, Milne J, Page GP, Somerville CR (2005) Identification of genes required for cellulose synthesis by regression analysis of public microarray data sets. Proc Natl Acad Sci USA **102:** 8633–8638

Potikha T, Delmer DP (1995) A mutant *of Arabidopsis thaliana* displaying altered patterns of cellulose deposition. Plant J **7:** 453–460

Potikha TS, Collins CC, Johnson DI, Delmer DP, Levine A (1999) The involvement of hydrogen peroxide in the differentiation of secondary walls in cotton fibers. Plant Physiol **119:** 849–858

R Development Core Team (2006) R: a language and environment for statistical computing. http://www.R-project.org

Reis D, Vian B (2004) Helicoidal pattern in secondary cell walls and possible role of xylans in their construction. C R Biol **327:** 785–790

Robert S, Mouille G, Höfte H (2004) The mechanism and regulation of cellulose synthesis in primary walls: lessons from cellulose-deficient Arabidopsis mutants. Cellulose **11:** 351–364

Scheible WR, Fry B, Kochevenko A, Schindelasch D, Zimmerli L, Somerville S, Loria R, Somerville CR (2003) An Arabidopsis mutant resistant to thaxtomin A, a cellulose synthesis inhibitor from *Streptomyces* species. Plant Cell **15:** 1781–1794

Schindelman G, Morikami A, Jung J, Baskin TI, Carpita NC, Derbyshire P, McCann MC, Benfey PN (2001) *COBRA* encodes a putative GPI-anchored protein, which is polarly localized and necessary for oriented cell expansion in Arabidopsis. Genes Dev **15:** 1115–1127

Schmid M, Davison TS, Henz SR, Pape UJ, Demar M, Vingron M, Scholkopf B, Weigel D, Lohmann JU (2005) A gene expression map of *Arabidopsis thaliana* development. Nat Genet **37:** 501–506

Sene C, McCann MC, Wilson RH, Grinter R (1994) Fourier-transform raman and Fourier-transform infrared spectroscopy (an investigation of five higher plant cell walls and their components). Plant Physiol **106:** 1623–1631

Shedletzky E, Shmuel M, Trainin T, Kalman S, Delmer D (1992) Cell wall structure in cells adapted to growth on the cellulose-synthesis inhibitor 2,6-dichlorobenzonitrile: a comparison between two dicotyledonous plants and a graminaceous monocot. Plant Physiol **100:** 120–130

Siedlecka A, Wiklund S, Péronne MA, Micheli F, Lesniewska J, Sethson I, Edlund U, Richard L, Sundberg B, Mellerowicz EJ (2008) Pectin methyl esterase inhibits intrusive and symplastic cell growth in developing wood cells of *Populus*. Plant Physiol **146:** 554–565

Somerville C, Bauer S, Brininstool G, Facette M, Hamann T, Milne J, Osborne E, Paredez A, Persson S, Raab T, et al (2004) Toward a systems approach to understanding plant cell walls. Science **306:** 2206–2211

Stamatakis A (2006) RAxML-VI-HPC: maximum likelihood-based phylogenetic analyses with thousands of taxa and mixed models. Bioinformatics **22:** 2688–2690

Svalheim O, Robertsen B (1993) Elicitation of hydrogen peroxide production in cucumber hypocotyl segments by oligo-1,4-alpha d-galacturonides and an oligo-beta-glucan preparation from cell walls of *Phytophthora megasperma* f. sp. *glycinea*. Physiol Plant **88:** 675–681

Taylor NG, Laurie S, Turner SR (2000) Multiple cellulose synthase catalytic subunits are required for cellulose synthesis in *Arabidopsis*. Plant Cell **12:** 2529–2540

Taylor NG, Scheible WR, Cutler S, Somerville CR, Turner SR (1999) The *irregular xylem3* locus of *Arabidopsis* encodes a cellulose synthase required for secondary cell wall synthesis. Plant Cell **11:** 769–780

Turner SR, Somerville CR (1997) Collapsed xylem phenotype of *Arabidopsis* identifies mutants deficient in cellulose deposition in the secondary cell wall. Plant Cell **9:** 689–701

Updegraff DM (1969) Semimicro determination of cellulose in biological materials. Anal Biochem **32:** 420–424

Upton C, Buckley JT (1995) A new family of lipolytic enzymes? Trends Biochem Sci **20:** 178–179

Vogel JP, Raab TK, Somerville CR, Somerville SC (2004) Mutations in *PMR5* result in powdery mildew resistance and altered cell wall composition. Plant J **40:** 968–978

Vorwerk S, Somerville S, Somerville C (2004) The role of plant cell wall polysaccharide composition in disease resistance. Trends Plant Sci **9:** 203–209

Wang H, Lockwood SK, Hoeltzel MF, Schiefelbein JW (1997) The ROOT HAIR DEFECTIVE3 gene encodes an evolutionarily conserved protein with GTP-binding motifs and is required for regulated cell enlargement in Arabidopsis. Genes Dev **11:** 799–811

Wong HL, Pinontoan R, Hayashi K, Tabata R, Yaeno T, Hasegawa K, Kojima C, Yoshioka H, Iba K, Kawasaki T, et al (2007) Regulation of rice NADPH oxidase by binding of Rac GTPase to its N-terminal extension. Plant Cell **19:** 4022–4034

Xin Z, Mandaokar A, Chen J, Last RL, Browse J (2007) Arabidopsis *ESK1* encodes a novel regulator of freezing tolerance. Plant J **49:** 786–799

Yoshida S, Ito M, Nishida I, Watanabe A (2001) Isolation and RNA gel blot analysis of genes that could serve as potential molecular markers for leaf senescence in *Arabidopsis thaliana*. Plant Cell Physiol **42:** 170–178

Zhong R, Kays SJ, Schroeder BP, Ye ZH (2002) Mutation of a chitinase-like gene causes ectopic deposition of lignin, aberrant cell shapes, and overproduction of ethylene. Plant Cell **14:** 165–179

Zhong R, Ye ZH (2004) Molecular and biochemical characterization of three WD-repeat-domain-containing inositol polyphosphate 5-phosphatases in *Arabidopsis thaliana*. Plant Cell Physiol **45:** 1720–1728

Zhong RQ, Morrison WH, Freshour GD, Hahn MG, Ye ZH (2003) Expression of a mutant form of cellulose synthase *AtCesA7* causes dominant negative effect on cellulose biosynthesis. Plant Physiol **132:** 786–795

Zhong RQ, Pena MJ, Zhou GK, Nairn CJ, Wood-Jones A, Richardson EA, Morrison WH, Darvill AG, York WS, Ye ZH (2005) *Arabidopsis fragile fiber8*, which encodes a putative glucuronyltransferase, is essential for normal secondary wall synthesis. Plant Cell **17:** 3390–3408

Zykwinska AW, Ralet MCJ, Garnier CD, Thibault JFJ (2005) Evidence for in vitro binding of pectin side chains to cellulose. Plant Physiol **139:** 397–407